

## Supplemental Information

# Biodegradable Viral Nanoparticle/Polymer Implants Prepared *via* Melt-Processing

Parker W. Lee<sup>†</sup>, Sourabh Shulka<sup>‡</sup>, Jaqueline D. Wallat<sup>†</sup>, Chaitanya Danda<sup>†</sup>, Nicole F.

Steinmetz<sup>‡†§||<sup>⊖</sup></sup>, Joao Maia<sup>†</sup>, Jonathan K. Pokorski<sup>†\*</sup>

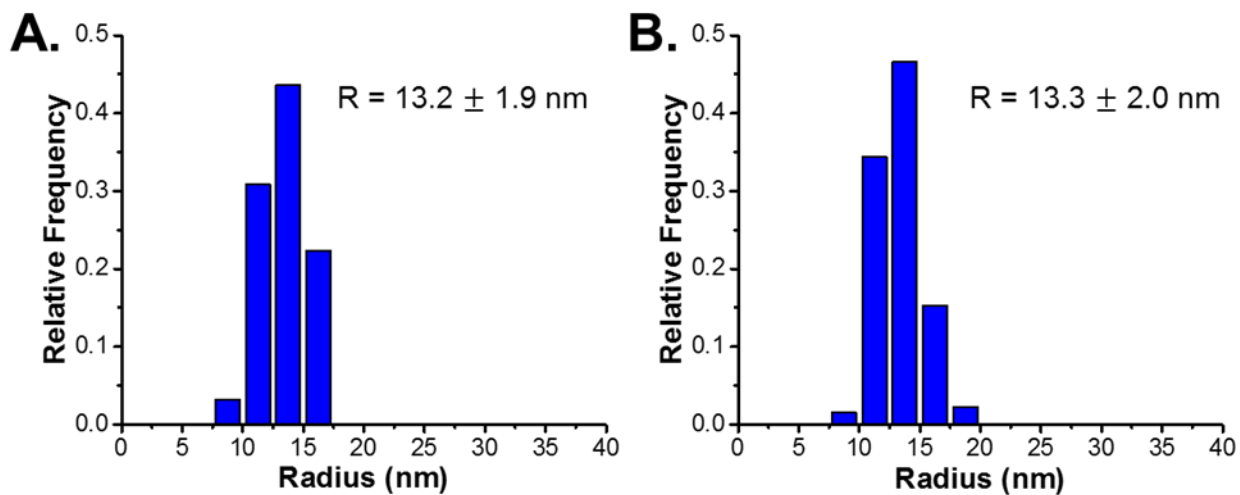
<sup>†</sup> Department of Macromolecular Science and Engineering, Case Western Reserve University, Case School of Engineering, Cleveland, Ohio 44106, United States

<sup>‡</sup> Department of Biomedical Engineering, Case Western Reserve University, Case School of Engineering, Cleveland, Ohio 44106, United States

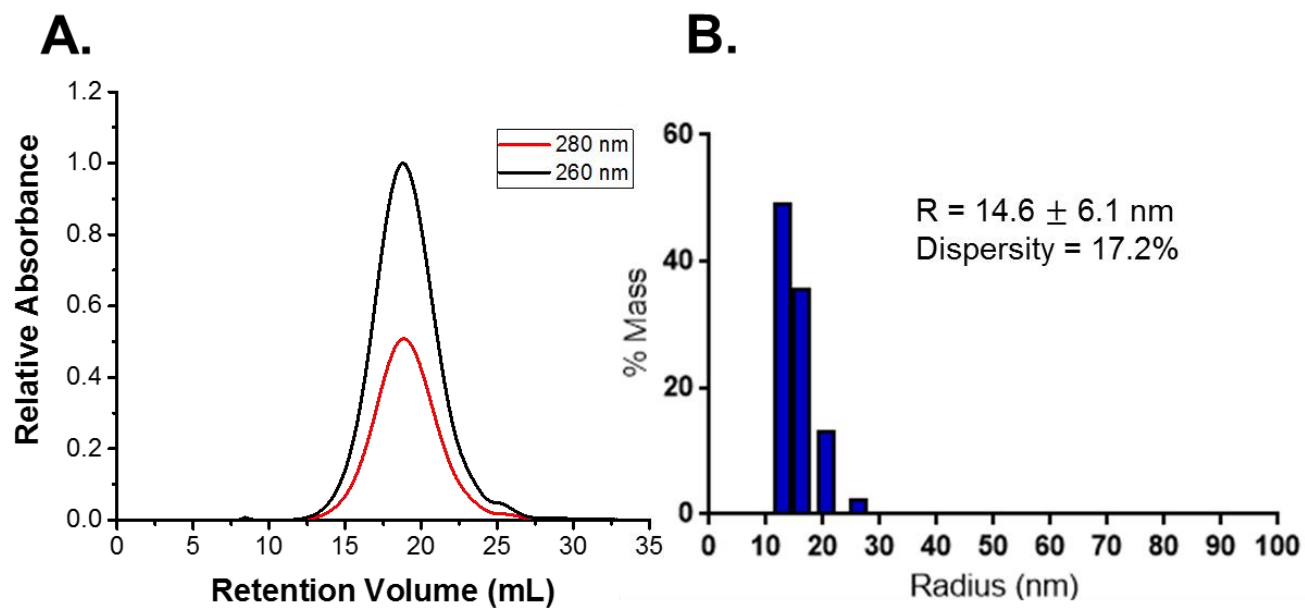
<sup>§</sup> Department of Radiology, Case Western Reserve University School of Medicine, Cleveland, Ohio 44106, United States

<sup>||</sup> Department of Materials Science and Engineering, Case Western Reserve University, Cleveland, Ohio 44106, United States

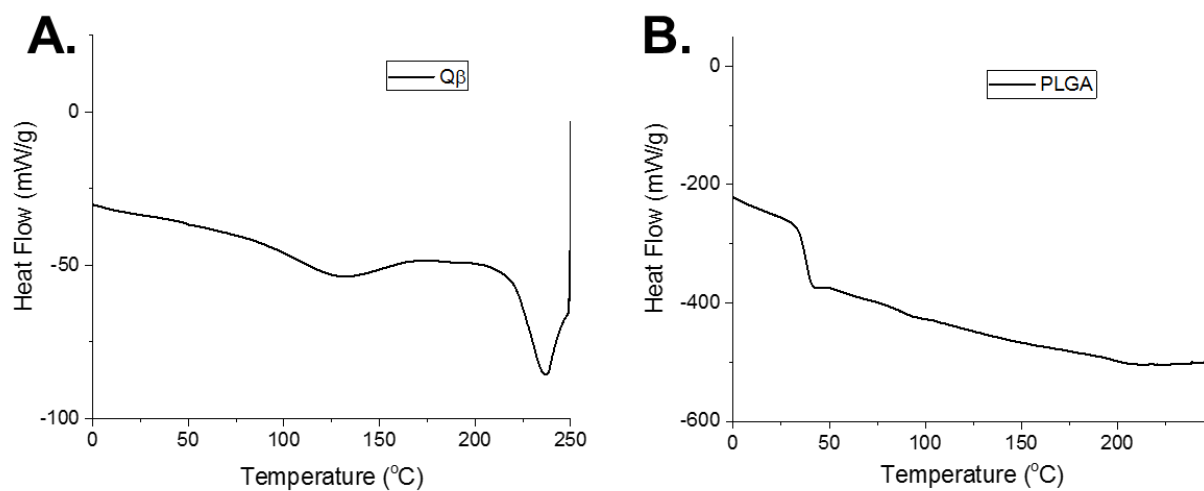
<sup>⊖</sup> Case Comprehensive Cancer Center, Division of General Medical Sciences-Oncology, Case Western Reserve University, Cleveland, Ohio 44106, United States



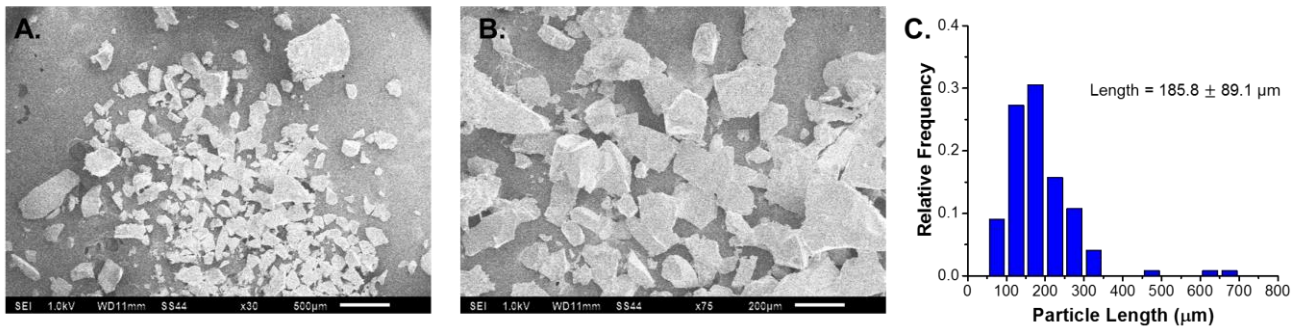
**Figure S1:** Size distribution histograms for (A.) Q $\beta$  and (B.) Q $\beta$  after melt processing as determined from the TEM micrographs using ImageJ analysis. The relative frequency plots are reported from measurements of at least 90 particles for both samples.



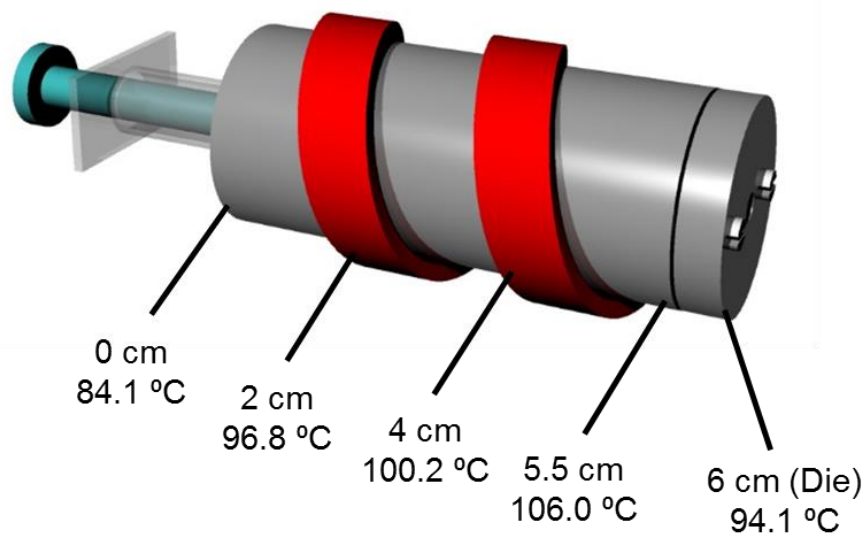
**Figure S2:** (A.) FPLC chromatogram and (B.) DLS histogram of lyophilized and re-suspended Q $\beta$ .



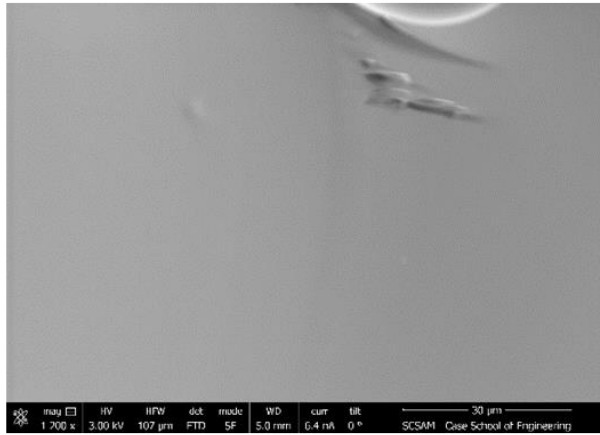
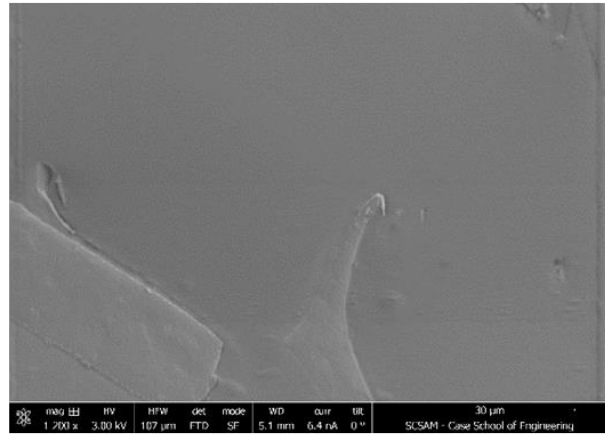
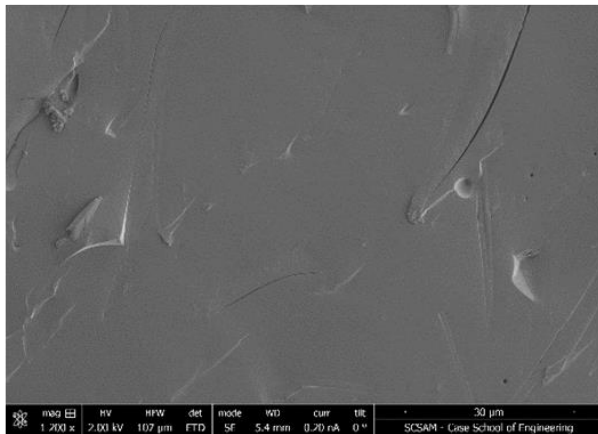
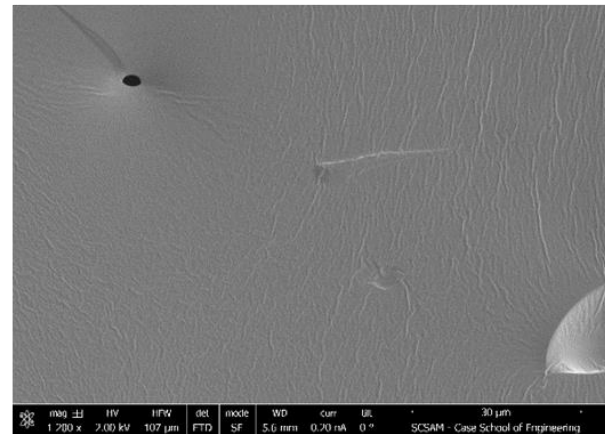
**Figure S3:** (A.) DSC thermogram of lyophilized Q $\beta$  and (B.) DSC thermogram of PLGA (first heating cycle shown, exotherm up).



**Figure S4:** SEM images of the ground PLGA particles used for melt-processing at (A.) 30X and (B.) 75X magnification. (C.) Relative frequency plots for the length of PLGA particles determined from both SEM images. The relative frequency plots are reported from measurements of at least 120 particles taken from both images and the length measurement is defined as the longest side of an individual particle.



**Figure S5:** Schematic of the temperature profile of the syringe-die extruder measured *via* an IR-thermometer. The overall temperature of the internal chamber of the extruder was 95 °C as measured *via* a glass thermometer.

**A.****B.****C.****D.**

**Figure S6:** SEM images of EDS map sites of (A.) neat PLGA, (B.) 1 wt% Q $\beta$ , (C.) 5 wt% Q $\beta$ , and (D.) 10 wt% Q $\beta$ .

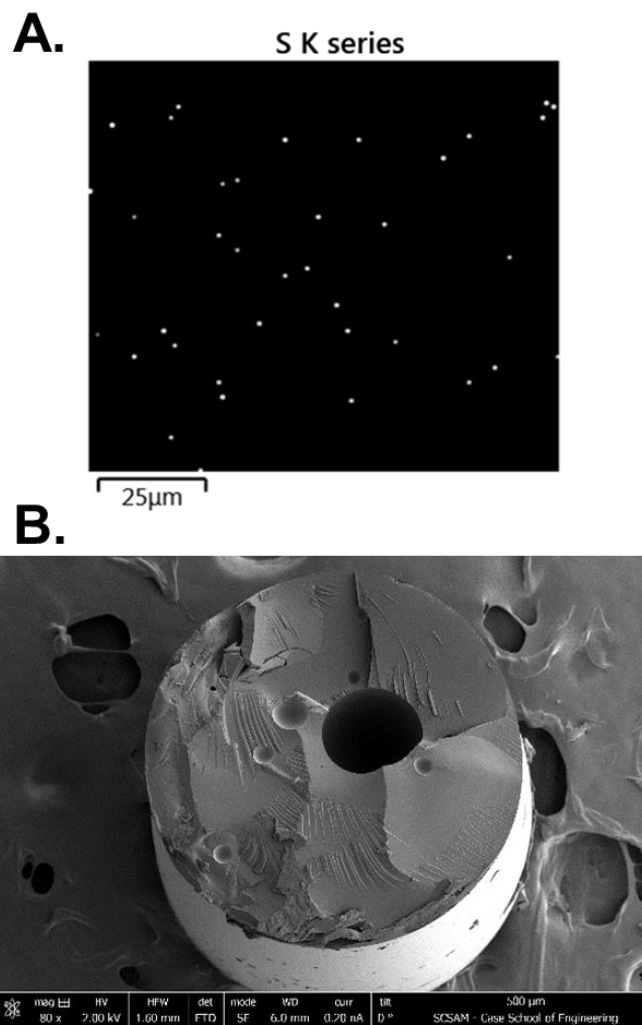


**Figure S7:** (A.) EDS sulfur signal map of neat PLGA cross-section. (B.) Full-scale SEM image neat PLGA cross-section.



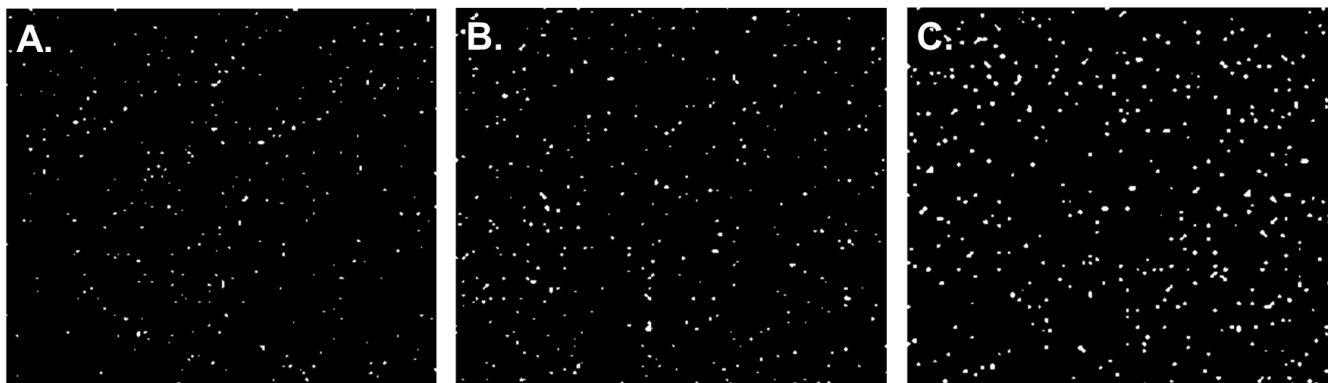


**Figure S8 :** EDS spectrum sulfur K-series emission signal map of (A.) 1 wt% Q $\beta$ , (B.) 5 wt% Q $\beta$ , and (C.) 10 wt% Q $\beta$  loaded PLGA material cross-sections that have been thresholded to 50% of the maximum signal intensity to highlight the difference in signal intensity between loading levels.

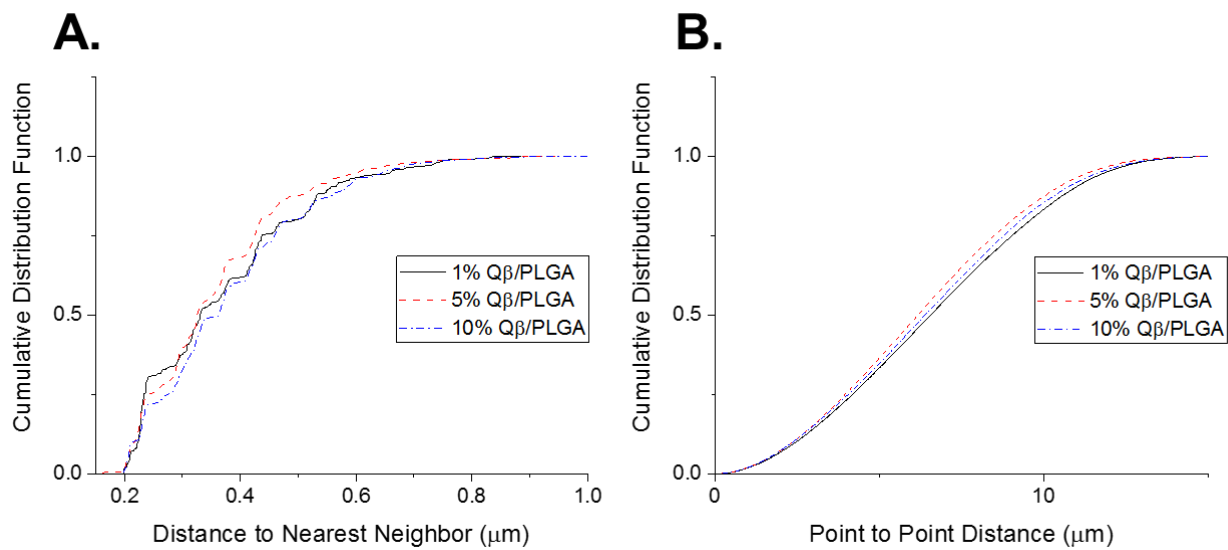


**Figure S9:** Quantitative dispersion cumulative distribution function plots of (A.) distance from particle to the nearest neighbor and (B.) distance from particle to another particle.

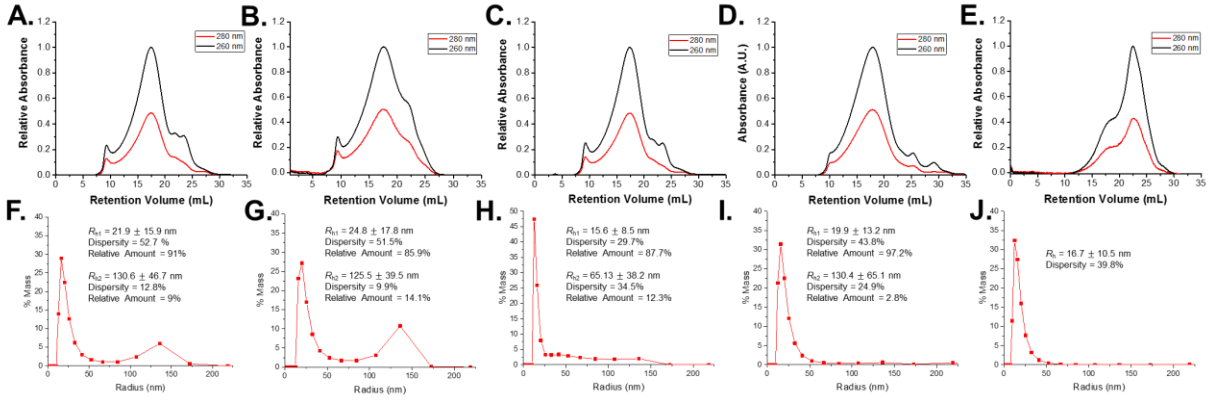


**Figure S10:** FPLC chromatograms of recovered Q $\beta$  samples subjected to shear rates of (A.) 0.25  $s^{-1}$ , (B.) 0.5  $s^{-1}$ , (C.) 2.5  $s^{-1}$ , (D.) 5  $s^{-1}$  and (E.) 25  $s^{-1}$ . DLS plots of recovered Q $\beta$  samples subjected to shear rates of (F.) 0.25  $s^{-1}$ , (G.) 0.5  $s^{-1}$ , (H.) 2.5  $s^{-1}$ , (E.) 5  $s^{-1}$  and (J.) 25  $s^{-1}$ .

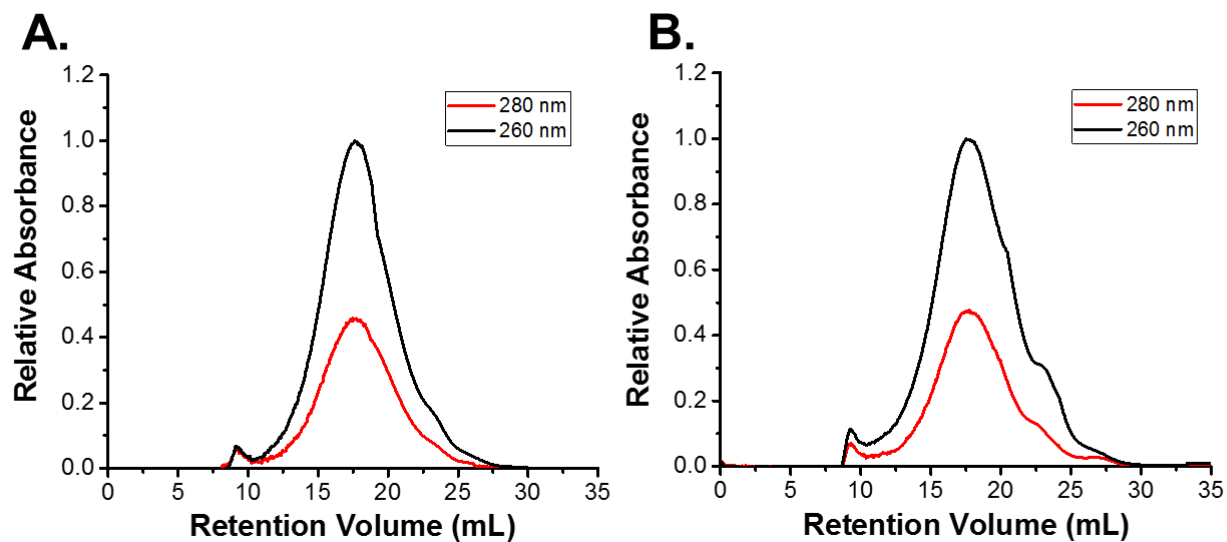


**Figure S11:** FPLC chromatograms of Q $\beta$  released from 10% Q $\beta$ /PLGA implants at (A) 2 days of release and (B) 50 days of release time points.

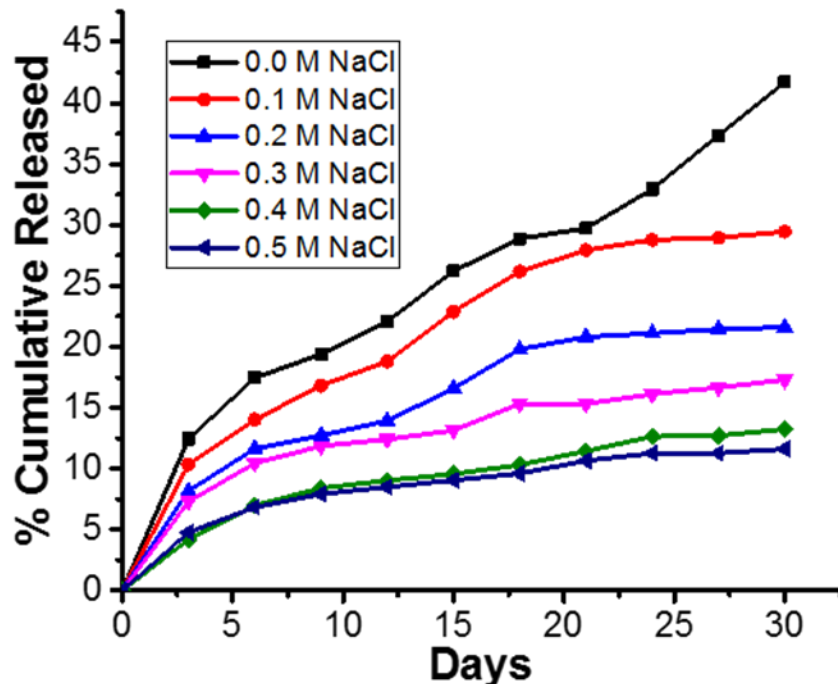


**Figure S12:** Release profiles of 10 wt% Q $\beta$  loaded PLGA samples 0.01 M phosphate buffer, pH 7.4, with increasing concentrations of NaCl.

**Table S1:** Percentage of Q $\beta$  released in response to sequential incubation for 3 days with 1 M

	NaCl Concentration					
	0.0 M	0.1 M	0.2 M	0.3 M	0.4 M	0.5 M
1 M NaCl	0.239%	0.039%	0.139%	0.633%	0.011%	0.160%
5 M GnCl	6.01%	7.44%	11.3%	23.3%	27.7%	28.1%
5 mM SDS	42.1%	50.5%	53.9%	51.1%	53.3%	52.9%

NaCl, 5 M GnHCl, and 5 mM SDS respectively.

## **Full Materials and Methods**

### Materials

Poly(lactic-*co*-glycolic acid) (EXPANSORB® 10P019, 50:50 PLGA, inherent viscosity 0.15-0.25 dl $g^{-1}$ , 5-20 kDa) was purchased from PCAS. Potassium phosphate monobasic anhydrous, potassium phosphate dibasic anhydrous, sodium phosphate dibasic heptahydrate, Gibco 1X PBS pH 7.4, butanol, Miller LB Broth, D-sucrose, guanidine hydrochloride, sodium dodecyl sulfate, and isopropyl  $\beta$ -D-1-thiogalactopyranoside, kanamycin, spectinomycin, sodium azide, ethyl acetate, neonatal calf serum, 1-step PNPP substrate, Tween-20, albumin standard, and sodium hydroxide were purchased from Fisher Scientific. Poly(ethylene glycol) ( $M_n = 20000$ ) was purchased from Alfa Aesar. Poly(ethylene glycol) ( $M_n = 8000$ ) was purchased from Amresco. Bradford reagent was purchased from VWR. Goat anti-mouse IgG-alkaline phosphatase antibody was purchased from Life Technologies. Goat anti-mouse IgG2a, IgG2b and IgG1-alkaline phosphatase antibodies were purchased from Novus Biologics. All reagents were used directly, without further purification.

### Instrumentation

Fast protein liquid chromatography (FPLC) was performed using a GE Healthcare AKTA-FPLC 900 chromatography system equipped with a Sephacryl 1000 SF 10/300 size exclusion column. For all FPLC experiments, the mobile phase was 50 mM phosphate buffer, with 150 mM NaCl (pH 7.4) at a flow rate of 0.4 mL/min. Samples were injected at a concentration of 0.1 – 0.75 mg/mL and the resulting chromatograms were normalized by the maximum absorbance at 260 nm. Dynamic light scattering (DLS) experiments were performed on a Wyatt DynaPro NanoStar

DLS instrument. Samples were analyzed at 25 °C in plastic disposable cuvettes with a path length of 10 mm. Transmission electron microscopy (TEM) was performed on a Zeiss Libra 200EF microscope. Negative stained TEM samples were mounted on 400 mesh hexagonal copper grids bearing Formvar support film, stained with 2% uranyl acetate solution, and allowed to dry for 12 h. Microplate measurements were taken with a Biotek Synergy HT microplate reader. Centrifugation was performed with an Eppendorf 5810 R centrifuge. Ultracentrifugation was performed with a Beckman Coulter Optima L-100 XP ultracentrifuge. SEM-EDS Imaging was performed using a Helios Nanolab 650 SEM combined with an Oxford X-Max 80 mm<sup>2</sup> Silicon Drift Detector XEDS system. Melt pressing was performed with a Carver Model C laboratory press. Shear application was performed with an Anton-Parr Physica MCR 501 rheometer. UV-vis spectra were collected using a Shimadzu BioSpecNano UV-vis spectrophotometer. Differential scanning calorimetry was performed using a TA Instruments Q100 DSC instrument. The temperature profile of the syringe-die extruder was measured using a Minolta Land Cyclops 330S infrared thermometer. Scanning electron microscopy was performed using a JEOL-6510LV scanning electron microscope at 1 kV.

## Methods

### *Q $\beta$ Expression and Purification*

Q $\beta$  was prepared based on a previously published protocol.<sup>1</sup> Chemically competent BL21(DE3) *E. coli* cells were transformed with pET28CP (containing the Q $\beta$  coat protein sequence) and plated onto lysogeny broth (LB) agar media containing kanamycin (50  $\mu$ g/mL). The following day, isolated colonies were picked from plates into 100 mL of autoclaved selective LB media and grown to saturation for 12 h at 37°C. A total of 10 mL of culture was

then diluted into 1000 mL of freshly prepared selective LB media. Culture growth was monitored by optical density at 600 nm (OD600). When the OD600 of the cultures reached approximately 0.8 (mid log phase), protein expression was induced with the addition of 10 mL of 100 mM IPTG, giving a final IPTG concentration of 1 mM. Shaking was continued at 37 °C for an additional 6 h, at which point cells were collected by centrifugation in an Eppendorf A-4-81 rotor at 4000 rpm (4°C) for 30 min. The supernatant was decanted, and the cell pellet was frozen at -80 °C until purification. Cells were then resuspended in ~100 mL of PBS, pH 7.4. The buffer used for the original resuspension continued to be used for subsequent steps of particle preparation. Samples were chilled on ice and then sonicated with a probe sonicator (10 min total sonication time, 5 s on and 5 s off, 60-70 W power output) in an ice bath to lyse cells. The cell debris was pelleted in an Eppendorf FA-45-6-30 rotor at 10000 rpm for 10 min, and the supernatant was decanted and collected. The Q $\beta$  particles were precipitated from the resulting supernatant by the addition of 10% w/v PEG8000 at 4°C for 12 h on a rotisserie. The precipitated fraction was isolated from the supernatant by centrifugation in an Eppendorf FA-45-6-30 rotor for 10 min (4°C) at 10,000 rpm. The pellet was redissolved in ~20 mL of PBS and extracted with a 1:1 v/v solution of n-BuOH/CHCl<sub>3</sub> to remove excess lipid. The aqueous fraction was collected following centrifugation using a FA-45-6-30 rotor for 10 min, 4 °C at 10000 rpm. Q $\beta$  particles were purified on 10-40% sucrose gradients in an SW28 rotor at 28000 rpm for 4 hours. Approximately 4 mL of light scattering Q $\beta$  solution was pulled from each gradient tube and subsequently pelleted in an ultracentrifuge (50.2Ti rotor, 42K, 3 h). The purified Q $\beta$  particles were dissolved in PBS (pH 7.4) and purity was verified *via* PAGE, FPLC, DLS, and TEM. Size distribution analysis of the TEM images was performed using ImageJ with



the measurement of at least 90 particles for one curve. A liter culture typically yielded ~100 mg of pure Q $\beta$ .

Q $\beta$  particles for immunology studies were prepared using electrocompetent ClearColi® BL21(DE3) *E. coli* (Lucigen) containing genes encoding for a mutant non-immunogenic lipopolysaccharide outer membrane component.<sup>2</sup> Cells were transformed with pCDFCP (containing the Q $\beta$  coat protein sequence) *via* electroporation. The Q $\beta$  particles were then prepared as previously described, using spectinomycin as the antibiotic and depyrogenated water and containers during the preparation. The yield of particles manufactured through this method was typically ~50% compared to standard BL21(DE3) cells.

Q $\beta$  particles were spin-filtered into deionized water using 100 kDa MWCO spin filters and frozen. The samples were then lyophilized for 3 days to yield a solid white powder. No adverse aggregation or particle breakup was observed after lyophilization and resuspension.

#### *Differential Scanning Calorimetry*

Differential scanning calorimetry (DSC) was performed using T-Zero hermetic aluminum pans under a nitrogen atmosphere. Lyophilized Q $\beta$  was analyzed from -50 to 250 °C with a heating rate of 20 ° C/min using a pinhole pan configuration. PLGA was analyzed from 0 ° C to 250 ° C with a heating rate of 20 ° C/min using a sealed pan configuration. Thermograms were normalized for sample weight and are reported with the exotherm up.

#### *Preparation of PLGA/Protein Implants*

Poly(lactic-*co*-glycolic acid) (PLGA), 8 kDa polyethylene glycol (8KPEG), and 20 kDa PEG (20KPEG) were individually ground manually with a mortar and pestle twice, 10 minutes

each time, into a fine powder. The PLGA powder consisted of particles with an average length of  $185.8 \pm 89.1 \mu\text{m}$  as determined *via* SEM image analysis. PLGA was mixed with the appropriate weight percent of lyophilized Q $\beta$  and PEG (if added) *via* repeated vortexing in a 2 mL Eppendorf tube. Formulations were as follows with all percentages expressed as a weight percent: PLGA/1%Q $\beta$ ; PLGA/1%Q $\beta$ /10%8KPEG; PLGA/1%Q $\beta$ /10%20KPEG, PLGA/5%Q $\beta$ , PLGA/10%Q $\beta$ . Two different custom built aluminum syringe-die were used for melt processing of the blends to minimize material input. Both syringe-die systems consisted of a cylinder with a circular 1 mm exit diameter that was wrapped with heating tape, combined with a digital control element to provide constant heating. The die used for melt encapsulation of samples for *in vitro* testing utilized polypropylene BD™ LUER LOK™ syringes which were filled with 500-200 mg of the PLGA/Q $\beta$  blends and heated at 95 ° C as determined by a glass thermometer (99.9 °C average along the temperature profile as determined *via* an infrared thermometer) for 10 minutes. The melted PLGA/Q $\beta$  blend was flowed through the die using a syringe pump with a velocity of 3 mm s<sup>-1</sup> (~2.35 mm<sup>3</sup> s<sup>-1</sup> volumetric flow rate) The resulting cylindrical implants had diameters ranging from 1.0-1.3 mm. Melt encapsulation of ClearColi® produced Q $\beta$  for *in vivo* testing was performed with a cylinder manufactured to fit polypropylene 1 mL volume Norm-Ject syringes. The die still consisted of a circular 1 mm hole. This barrel was used to minimize materials due to the lower yield of ClearColi® produced particles. The syringe was filled with 50-100 mg of the appropriate PLGA/Q $\beta$  blend and extruded in the same method as previously described. There was no difference observed in implant diameter or particle integrity between samples fabricated with different barrels.

#### *Q $\beta$ Extraction from Implants*

Rapid Q $\beta$  recovery from implants was performed by dissolving ~100 mg in 2 mL of ethyl acetate for 2 hours. This was followed by centrifugation for 10 minutes at 10,000 rpm using an Eppendorf 5810 R centrifuge with a fixed angle rotor, based on a previously established protocol for organic extraction of active lysozyme.<sup>3</sup> The supernatant was decanted and the process was repeated two more times. The remaining solids were dried under vacuum at room temperature for 24 hours. The solid protein recovered was resuspended in PBS for 24 hours at 4°C and analyzed *via* FPLC, DLS, and TEM.

#### *EDS-SEM and Image Analysis*

Distribution of Q $\beta$  in the implant cross section was determined by mapping the characteristic X-ray peak of sulfur. Samples were freeze-fractured and sputter coated with a 100 nm thick layer of palladium. Elemental spectra were collected at 5 kV for 15 minutes. Dispersion analysis was performed using ImageJ with the 3D ImageJ Suite.<sup>4-6</sup>

#### *Melt Pressing*

Melt pressing was performed with ~250 mg of PLGA/1%Q $\beta$  extruded samples. The samples were placed between two sheets of teflon coated aluminum foil and pressed at 100°C and 1500 psi for 5 minutes. The pressed samples were removed from the sheet and the Q $\beta$  was recovered and analyzed *via* the extraction method previously described.

#### *Shear Application*

Shear application was performed by loading 150-300 mg of PLGA/1%Q $\beta$  onto a 25 mm wide parallel plate rheometer at 95°C. Samples were allowed to equilibrate for 5 minutes, then

the top plate was lowered to a gap of 0.45 mm and shear rates from 0.1 - 50 s<sup>-1</sup> were applied for 3 minutes. The sample was recovered from the rheometer post-shear and the Qβ was recovered and analyzed *via* the extraction method previously described. The viscosity of the samples was also measured during this process and found to be in the range of 120-130 Pa·s, with an average of 128 Pa·s.

### *Radius Shear Dependency and Peclet Number Calculations*

Qβ samples recovered post-shear application were analyzed *via* DLS and FPLC. Weight average hydrodynamic radii were calculated from the DLS data for samples subjected to 0.1, 0.25, 0.5, 1, 2.5, 5, 10, 25, and 50 s<sup>-1</sup>. Samples subjected to 25 and 50 s<sup>-1</sup> exhibited extensive particle breakup when analyzed *via* FPLC. The breakup product was assumed to be coat protein dimers, which exhibit a radius of 3.21 nm estimated from the crystal structure (PDB: 1QBE).<sup>7</sup> This estimate is similar to the hydrodynamic radius of green fluorescent protein (2.8 nm), which is of similar molecular weight to the coat protein dimer (27 and 28 kDa respectively).<sup>8</sup> The ratio of intact particles to coat protein dimers was calculated *via* curve fitting of the two major curves observed in the FPLC. The ratio of intact particles was multiplied by the weight average radius determined *via* DLS and added to the ratio of coat protein dimer multiplied by 3.21 nm to give an average radius of species in the 25 and 50 s<sup>-1</sup> samples, as shown by the equation below.

$$R_{Ave} = (R_{Ave,DLS}) * (\%_{Particle}) + (3.21 \text{ nm}) * (\%_{Dimer})$$

Where:  $R_{ave}$  = average radius for samples subjected to 25 and 50 s<sup>-1</sup> shear rates

$R_{Ave, DLS}$  = mass average radius calculated from the DLS result

$\%_{Particle}$  = percentage of particle calculated from curve fitting of the FPLC result

$\%_{\text{Dimer}}$  = percentage of dimer calculated from curve fitting of the FPLC result

The weight average radius was divided by the weight average radius of Q $\beta$  that had been extracted from PLGA/1%Q $\beta$  samples that had not been subjected to shear. This result was plotted as the radius of shear applied samples to the initial radius *versus* shear rate.

This result was non-dimensionalized by calculating the Peclet number for each shear rate. The Peclet number (Pe) is a dimensionless number of the ratio of convective forces vs the diffusive forces in a fluid system. The Peclet number was calculated as the ratio of shear stress applied on the particles over the diffusive forces estimated by the Stokes-Einstein equation, as shown by the equation below.

$$Pe = \frac{6\pi\eta\dot{\gamma}R^3}{k_bT}$$

Where:  $\eta$  = viscosity of the polymer melt (Pa·s)

$\dot{\gamma}$  = shear rate applied to the system ( $s^{-1}$ )

R = weight average radius of the particles before shear application (m)

$k_b$  = Boltzmann's constant ( $J\cdot K^{-1}$ )

T = temperature of the system (K)

The resulting plot of particle radius of shear applied samples to the initial radius *versus* Peclet number is useful in relating the aggregation behavior of Q $\beta$  during melt encapsulation to other polymer systems with different viscosities and processing temperatures. Furthermore, computational analysis has revealed the aggregation behavior of colloidal spheres follows a universal trend when plotted against the Peclet depletion number ( $Pe_{\text{dep}}$ ).<sup>9</sup> This approach can be directly applied to the results with melt-encapsulated Q $\beta$  subjected to applied shear, where Q $\beta$

functions as a solid colloidal particle within a viscous PLGA matrix. The  $Pe_{dep}$  takes into account the attractive or repulsive forces between particles through incorporation of an interaction potential and an interaction length-scale, whereas the  $Pe$  assumes a hard sphere model with no interactive forces. The formula for  $Pe_{dep}$  is given below, where all previously defined variables are the same.

$$Pe_{dep} = \frac{12\pi\eta\dot{\gamma}R^3\xi}{Ck_bT}$$

Where:  $\xi$  = interaction length-scale between particles

$C$  = interaction potential

Previous computational analysis demonstrated that the break-up of colloidal aggregates occurs at a  $Pe_{dep}$  value of 1 for all colloidal systems. The plot of weight average radius ratio *versus*  $Pe$  yields a maximum peak value before radius decrease of  $Pe = 2.6$ . Assuming that the system follows the behavior observed computationally, this  $Pe$  value can be shifted to a  $Pe_{dep} = 1$  on the universal curve and allow for the calculation of the interaction potential between  $Q\beta$  particles during shear application under melt processing conditions. The  $\xi$  value is assumed to be 0.1 based on only short range interactions between the particles due to the low volume fraction of the particles. Using this assumption, the critical value  $Pe = 2.6$  was set equal to a  $Pe_{dep} = 1$  as shown below.

$$\frac{Pe}{Pe_{dep}} = \frac{2.6}{1} = \frac{\left(\frac{6\pi\eta\dot{\gamma}R^3}{k_bT}\right)}{\left(\frac{12\pi\eta\dot{\gamma}R^3\xi}{Ck_bT}\right)}$$

Solving this equation for C yields  $C \approx 0.5$ , indicating a weak interaction potential between Q $\beta$  particles in the melt state.

### *Shear Application Thermal Analysis Calculations*

Mathematical analysis was performed to estimate the total applied energy to the system during shear application and correlate it to the observed particle breakup. Q $\beta$  particle breakup into free dimers involves the breakage of disulfide bonds between adjoining dimers on the particle, with each dimer containing 4 disulfide linkages and one particle containing 90 coat protein dimers. The bond dissociation energy of a disulfide bond is typically 251 kJ/mol. Thus, the theoretical energy of all disulfides per particle was calculated to be 45,180 kJ/mole of particle. Integration of the first endothermic peak on the DSC thermogram (from 84 to 172°C) as shown by the equation below, which is speculated to be disulfide breakup, yielded a value of 43,860 kJ/mol particle in good agreement with the theoretical value.<sup>10,11</sup>

$$E_{disulfide} = (MW_{Q\beta}) \left( \frac{\Delta T}{s} \right)^{-1} \int_{T_1}^{T_2} \left( \frac{W}{g} \right) dT$$

Where:  $E_{disulfide}$  = total enthalpy of disulfides per mole of particle (J/mol Q $\beta$ )

$MW_{Q\beta}$  = molecular weight of Q $\beta$  = 2,556,000 g/mol

$\Delta T/s$  = heating rate of the DSC study, 0.333 K/s

$mW/g$  = heat flux of the DSC sample per gram (W/g)

The value determined *via* DSC integration was used to calculate the total disulfide bond energy present based on the mass of Q $\beta$  present in each shear application sample. The moles of PLGA in the system was calculated based on the mass of PLGA in the system and an average molecular weight of 12.5 kDa.

The total applied energy to the system during shear application was calculated as the sum of the energy applied by shear stress and thermal energy with the effects of shear heating taken into account utilizing the equations shown below. The energy values were normalized by the total disulfide bond energy present in each sample.

$$E_{shear} = \eta \dot{\gamma} V_{system}$$

$$E_{thermal} = k_b N_A (T_{applied} + \Delta T_{shear}) (mol_{Q\beta} + mol_{PLGA})$$

Where:  $\eta$  = viscosity of the polymer melt (Pa·s)

$\dot{\gamma}$  = shear rate applied to the system ( $s^{-1}$ )

$V_{system}$  = total volume of Q $\beta$  and PLGA ( $m^3$ )

$k_b$  = Boltzmann's constant ( $J \cdot K^{-1}$ )

$N_A$  = Avagadro's number

$T_{applied}$  = temperature during shear application (K)

$\Delta T_{shear}$  = temperature increase due to shear heating (K)

$mol_{Q\beta}$  = moles of Q $\beta$  in the system

$mol_{PLGA}$  = moles of PLGA in the system

### *Release studies*

Release studies assessing the impact of PEG additive and loading level were conducted on samples of the melt processed implants (~1.5 cm long, ~18 mg, n=3) for all samples. Samples were placed in dram vials with 0.5 mL of Gibco 1X PBS (pH 7.4, 0.01 M phosphate, 0.137 M NaCl, 0.0027 M KCl) with 0.01 wt% sodium azide and incubated at 37°C with 90% relative humidity. Aliquots of 0.45 mL were removed at each time point and replaced with fresh buffer.



Release studies assessing the impact of ionic strength and interactions between Q $\beta$  and PLGA were conducted on samples of melt processed implants containing 10 wt% Q $\beta$  (~1.5 cm long, ~18 mg). Samples were placed in dram vials with 0.5 mL of 0.1 M phosphate buffer (pH 7.4) and either 0.0, 0.1, 0.2, 0.3, 0.4, or 0.5 M NaCl and incubated under the same conditions as previous release samples. Aliquots of 0.45 mL were removed at each time point and replaced with the appropriate buffer. The release medium was changed to 0.1 M phosphate buffer with 1 M NaCl on day 30, 0.1 M phosphate buffer with 5 M guanidine hydrochloride on day 33, and 0.1 M phosphate buffer with 5 mM sodium dodecyl sulfate of day 35 to assess interparticle and particle-polymer interactions. The Q $\beta$  concentration at each time point was determined *via* Bradford assay with comparison to a freshly prepared bovine serum albumin standard curve. The release study was stopped when the implants were completely degraded and dissolved.

#### *Immunization and ELISA Analysis*

All experiments were carried out in accordance with Case Western Reserve University's Institutional Animal Care and Use Committee. Prior to immunization studies, 3 male Balb/c mice (Charles River) aged 7 weeks were implanted *subcutaneously* with ~0.5 cm of neat PLGA cylinder *via* puncture with a 16 gauge needle and insertion with forceps. The mice were monitored for 4 weeks and exhibited swelling at the site of insertion for 2 weeks after insertion, which subsequently subsided. The mice did not exhibit any adverse health or behavioral response to the implantation of the neat PLGA cylinders. For standard immunization, male Balb/c mice (Charles River) aged 7 weeks (n=5) were immunized 3 times on days 0, 14, and 28 with 50  $\mu$ g Q $\beta$  in 100  $\mu$ L sterile PBS through *subcutaneous* injections behind the neck using a 29G insulin syringe. The Q $\beta$  was produced in ClearColi *E. coli* cells that contain a modified

lipopolysaccharide (LPS) outer membrane that does not elicit an immune response in mice. Blood (~100  $\mu$ L) was drawn prior to the first immunization and on a weekly to biweekly basis *via* the retro-orbital plexus using heparinized capillary tubes and collected in Greiner Bio-One VACUETTE™ MiniCollect™ tubes. Serum was separated by centrifuging blood samples at 14,800 rpm, 4°C, for 10 min and stored at 4°C until analyzed *via* enzyme-linked immunosorbent-assay (ELISA). For implant immunization, male Balb/c mice (Charles River) aged 7 weeks (n=5) had 0.5 cm (~8 mg) of PLGA/10%Q $\beta$  inserted into the *subcutaneous* space on the neck *via* puncture with the tip of a 16 gauge needle and insertion with forceps. The amount of implanted material was chosen to deliver roughly the same amount of Q $\beta$  over the first 28 days as the mice immunized *via subcutaneous* injection based on the *in vitro* release profile, with ~0.8 mg of implant correlating to ~150  $\mu$ g of released Q $\beta$  over 30 days. Orbital bleeds were conducted as previously described on the same days as the standard immunization schedule mice. All mice were boosted at day 65 with 50  $\mu$ g of Q $\beta$ . After day 75, all mice were euthanized and the *subcutaneous* space was examined. No implant material was present in any of the implanted mice and no extensive scar tissue was present compared to non-implanted mice.

The anti-Q $\beta$  IgG response was measured by first coating Nunc Maxisorp 96-well plates with 2  $\mu$ g of Q $\beta$  in 200  $\mu$ L of sterile PBS, pH 7.4 at 4 ° C overnight. The wells were then blocked with 200  $\mu$ L of blocking buffer (2.5% w/v dry milk, 25% neonatal calf serum in PBS, pH 7.4) at 37 ° C for 1 hour. The wells were then incubated with mouse sera at dilutions from 1:100 to 1:1000000 in 100  $\mu$ L blocking buffer for 2 hours at 37 ° C. The wells were then incubated with 100  $\mu$ L of a 1:1000 dilution in blocking buffer of alkaline-phosphatase labeled goat anti-mouse IgG for 1 hour at 37 ° C. The wells were washed between each incubation step using 3X 250  $\mu$ L of 0.1% w/v Tween-20 in PBS, pH 7.4. The wells were developed using 100

μL of 1-step PNPP substrate at 4 ° C for 10 minutes. The reaction was stopped with 100 μL of 2 M NaOH and the absorbance was read at 405 nm in triplicate for each sample. The end-point titer value was determined comparison to a statistically defined cutoff value based on the pre-bleed measurements of 10 mice and a confidence level of 99%.<sup>12</sup> Values are expressed as the average and standard deviation of 5 mice.

Murine anti-Qβ IgG subtypes were determined *via* the ELISA method described above with alkaline-phosphatase labeled goat anti-mouse IgG1, IgG2a, and IgG2b used for detection. Percentages are expressed as the average and standard deviation of 5 mice.

## References

- (1) Isarov, S. A.; Lee, P. W.; Pokorski, J. K. “Graft-To” Protein/Polymer Conjugates Using Polynorbornene Block Copolymers. *Biomacromolecules* **2016**, *17*, 641–648.
- (2) Mamat, U.; Wilke, K.; Bramhill, D.; Schromm, A. B.; Lindner, B.; Kohl, T. A.; Corchero, J. L.; Villaverde, A.; Schaffer, L.; Head, S. R.; *et al.* Detoxifying Escherichia Coli for Endotoxin-Free Production of Recombinant Proteins. *Microb. Cell Factories* **2015**, *14*, 57.
- (3) Ghalanbor, Z.; Körber, M.; Bodmeier, R. Improved Lysozyme Stability and Release Properties of Poly(lactide-Co-Glycolide) Implants Prepared by Hot-Melt Extrusion. *Pharm. Res.* **2010**, *27*, 371–379.
- (4) Schneider, C. A.; Rasband, W. S.; Eliceiri, K. W. NIH Image to ImageJ: 25 Years of Image Analysis. *Nat. Methods* **2012**, *9*, 671–675.
- (5) Andrey, P.; Kiêu, K.; Kress, C.; Lehmann, G.; Tirichine, L.; Liu, Z.; Biot, E.; Adenot, P.-G.; Hue-Beauvais, C.; Houba-Hérin, N.; *et al.* Statistical Analysis of 3D Images Detects

- Regular Spatial Distributions of Centromeres and Chromocenters in Animal and Plant Nuclei. *PLoS Comput. Biol.* **2010**, *6*, e1000853.
- (6) Ollion, J.; Cochenec, J.; Loll, F.; Escudé, C.; Boudier, T. TANGO: A Generic Tool for High-Throughput 3D Image Analysis for Studying Nuclear Organization. *Bioinformatics* **2013**, *29*, 1840–1841.
- (7) Golmohammadi, R.; Fridborg, K.; Bundule, M.; Valegård, K.; Liljas, L. The Crystal Structure of Bacteriophage Q Beta at 3.5 Å Resolution. *Struct. Lond. Engl. 1993* **1996**, *4*, 543–554.
- (8) Baum, M.; Erdel, F.; Wachsmuth, M.; Rippe, K. Retrieving the Intracellular Topology from Multi-Scale Protein Mobility Mapping in Living Cells. *Nat. Commun.* **2014**, *5*, 4494.
- (9) Boromand, A.; Jamali, S.; Maia, J. M. Structural Fingerprints of Yielding Mechanisms in Attractive Colloidal Gels. *Soft Matter* **2017**, *13*, 458–473.
- (10) Mukhopadhyay, R.; K. De, S.; Chakraborty, S. N. Effect of Vulcanization Temperature and Vulcanization Systems on the Structure and Properties of Natural Rubber Vulcanizates. *Polymer* **1977**, *18*, 1243–1249.
- (11) Xu, Y.; Chen, D. A Novel Self-Healing Polyurethane Based on Disulfide Bonds. *Macromol. Chem. Phys.* **2016**, *217*, 1191–1196.
- (12) Frey, A.; Di Canzio, J.; Zurakowski, D. A Statistically Defined Endpoint Titer Determination Method for Immunoassays. *J. Immunol. Methods* **1998**, *221*, 35–41.